

# Multidimensional Gas Turbine Combustion Modeling: Applications and Limitations

Hukam C. Mongia

*General Motors Corporation, Indianapolis, Indiana*

and

Robert S. Reynolds and Ram Srinivasan

*The Garrett Turbine Engine Company, Phoenix, Arizona*

## I. Introduction

A TYPICAL empirical gas turbine combustor design and development approach is based on extensive use of an experience data base and empirical (semianalytical) correlations along with extensive component and subcomponent testing. Such an approach has historically been fairly successful in developing combustors based on proved design concepts. Empirical methods exhibit limitations in a number of critical areas, some of which are:

- 1) Empirically based design methods have shown severe limitations in scaling combustors.
- 2) If significantly big jumps are required in the technology levels (e.g., combustor temperature rise, cycle pressure ratio, combustor performance, and durability levels), combustion engineers are hesitant to use empirical correlations based on an available experimental data base.
- 3) The applicability of experience correlations (developed for a certain design concept) is quite limited for some other novel or revolutionary combustion concepts.
- 4) With ever exacting design requirements of advanced technology combustors (combustor operating conditions, wide operability, low smoke, and significantly improved durability characteristics), better tools are needed to achieve an optimum solution to satisfy conflicting combustor design requirements.

The first extensive effort to develop and demonstrate an empirical/analytical combustor design methodology was initiated by the U.S. Army Research and Technology Laboratories in 1975. This technique was successfully applied in the design and development testing of two full-scale

small reverse-flow annular combustors.<sup>1</sup> Simultaneously, this new methodology was being used and refined under the NASA Pollution Reduction Technology Program. How this method was used for the design and development testing of a premix/prevaporized combustor is described in Ref. 2. In parallel with these two efforts, the empirical/analytical design procedure was being used for developing a ceramic combustor, which needed to have significantly lower wall temperature gradients for structural durability.<sup>3,4</sup>

Subsequent to successful applications of the empirical/analytical combustor design methodology, a number of advanced technology combustors have been developed with the aid of analytical models, as described in Sec. III. Section II describes the methodology. Although the method has been useful in providing design guidance, the model limitations are evident in regard to accuracy of the state-of-the-art numerics and physical submodels of turbulence, turbulence/chemistry interaction, spray evaporation/mixing, soot formation/oxidation, and radiation. Some of these deficiencies are discussed in Secs. IV and V.

## II. Multidimensional Combustion System Design Methodology

In the Army Combustor Design Criteria Validation Program,<sup>5,6</sup> the methodology was developed for designing small reverse-flow annular combustors. The gas turbine combustor flowfield analysis involved calculations for the flow around the combustor liner and within the reverse-flow combustion chamber, as shown in Fig. 1. The airflow around the combustor liner is calculated by a one-dimensional annulus flow

---

Hukam C. Mongia is the Chief of Combustors and Advanced Turbomachinery in the Allison Gas Turbine Division. Previously, Dr. Mongia worked in the Garrett Turbine Engine Company in Phoenix, where he was intensively involved in the development and application of analytical models as well as the design and development testing of a number of advanced and production combustion systems.

Robert C. Reynolds is an Engineering Specialist in the Aero/Thermo Component Design Division. He has been involved in the development and validation of three-dimensional combustion numerical models including evaluation of advanced numerics and turbulence models. Mr. Reynolds has also been responsible for the design and rig test evaluation of advanced combustion systems. He received his BSME degree from Purdue University in 1972.

Ram Srinivasan is a Supervisor in Combustion Engineering Sciences. In the seven years he has been employed at Garrett, he has been responsible for experimental and analytical efforts associated with advancements in combustor modeling. He was previously employed at the University of Houston where he was involved in research on thermal energy storage. He received his Ph.D. degree in aerospace engineering from Georgia Tech in 1977.

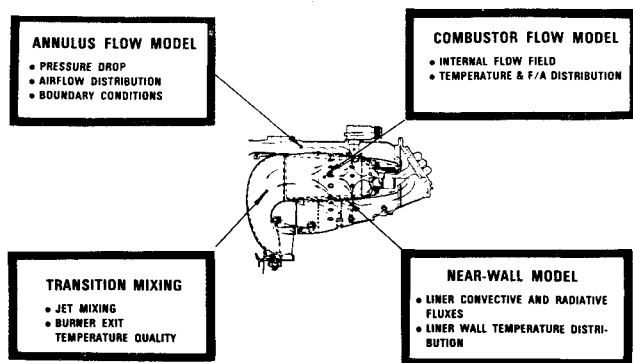


Fig. 1 Reverse-flow combustion system flow models.

model. This simple model has been adequate for reverse-flow combustor flow annuli. The annulus flow model calculates the pressure drop and airflow distribution around the combustor liner, in addition to calculating the liner boundary conditions required by the combustor flow model.

The combustor internal flowfield is calculated by two- or three-dimensional combustor flow models. The calculations include internal profiles of temperature, fuel:air ratios, and major chemical species. Special versions of the combustor flow models are used for predicting mixing in the transition liner where the main flow negotiates a full 180 deg bend. Due to computer memory limitations and the need to keep the required computer time affordable, separate programs are needed for predicting the flow near the liner walls if accurate convective and radiative heat loading levels are desired.

To develop novel combustion concepts and to incorporate promising concepts into future advanced in-line combustion systems, a more thorough understanding is needed for the flows in the combustor diffuser, annuli, and other important zones. A typical in-line gas turbine combustion system (see Fig. 2) requires improved models for the diffuser and annulus flow, nozzle/swirler flow interaction, primary and secondary zones, and liner near wall.

To design short low-loss stable diffusion systems for future high  $\Delta T$ , high  $M_3$  applications, an improved diffuser design methodology is needed.<sup>7</sup> Multidimensional, fully viscous codes and a time-efficient viscous/inviscid flow code are being developed for predicting flow and losses in the combustor prediffuser and annuli.

For high-performance, high-heat-release combustors with invisible exhaust smoke, the fuel nozzle flowfield characteristics, injection processes, fuel/air mixing, interaction with dome swirlers, and other flow features must be accurately predicted to achieve an optimum combustion system within a reasonable number of hardware iterations. This is accomplished by an empirical/analytical design methodology.

A generic methodology is described that is applicable for can, can-annular, and annular (straight through-flow or reverse flow) combustion systems. As shown by the wire diagram (see Fig. 3), the approach can be broadly divided into three steps. Given an engine cycle and mission requirements, combustor preliminary design is accomplished by using historical trend lines and empirical correlations augmented by simple (zero and one-dimensional) models. This phase of activities is strongly interactive with other engine components, including the compressor and turbine. The fuel injection system design is strongly influenced by combustor design requirements, as well as engine fuel scheduling and control logic.

Subsequent to the combustor preliminary design phase, an exhaustive empirical/analytical design effort is undertaken to satisfy many combustion design goals. These goals include combustion efficiency; pressure drop  $\Delta P$ ; smoke, lean

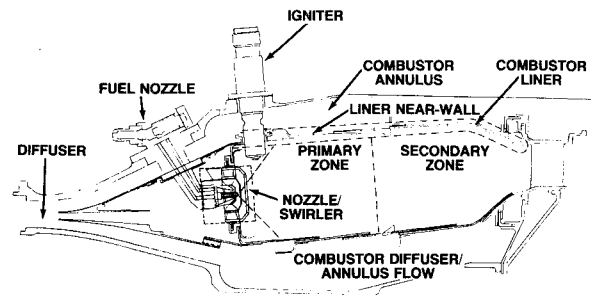


Fig. 2 In-line combustion system and flow regions.

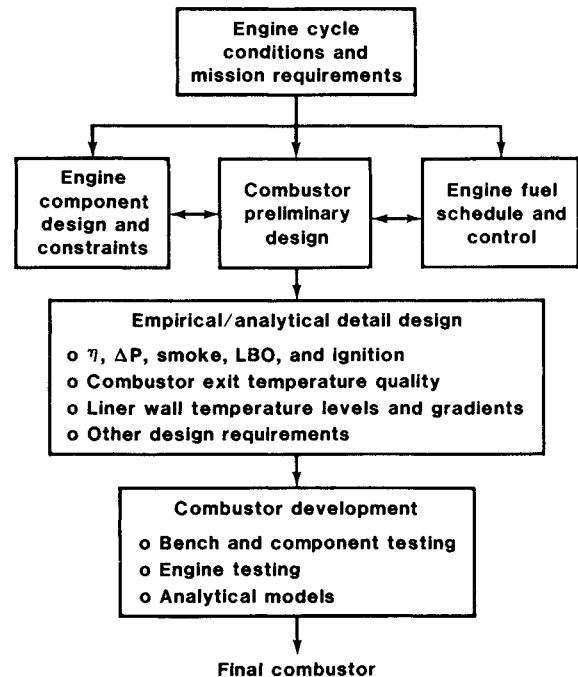


Fig. 3 Typical empirical/analytical combustor design logic diagram.

blowout (LBO), and ignition characteristics; combustor exit temperature quality; liner wall temperature levels/gradients; and other design requirements (weight, complexity, maintainability, etc.). Various empirical and analytical models are used during this phase to ensure that good design judgments are made for achieving the goals with minimal hardware iterations.

During the combustor development phase, a judicious combination of bench-scale testing, component testing, engine testing, and analytical models is used, leading to an acceptable final combustion system. The number of hardware iterations needed before one achieves the desired goals depends on many considerations. In spite of the known deficiencies in current state-of-the-art combustion modeling and numerics for complex gas turbine combustor flowfields, the qualitative insight provided by the analytical models is considered to be a prime factor for reducing development iterations of a number of advanced combustors, as described in the following section.

### III. Application as a Design Tool

A number of advanced technology combustors have been designed over the years with the help of multidimensional models. Some of these combustors are described briefly in this section. Two reverse-flow small annular combustors (see Figs. 4 and 5) were designed and tested under the Army Combustor Design Criteria Validation Program.<sup>1,5</sup> Both of

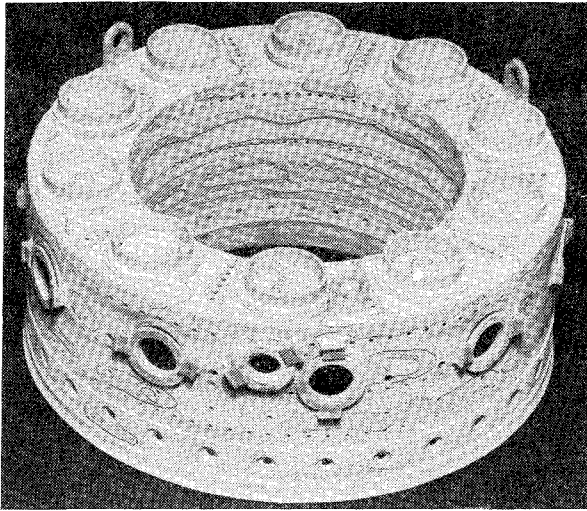


Fig. 4 U.S. Army Concept I liner paint run at sea-level, hot-day maximum power point ( $P_{13}=8.69$  atm,  $T_3=704^\circ\text{F}$  (647 K),  $T_4=2407^\circ\text{F}$  (1593 K),  $\Delta P/P_1=2.3\%$ ,  $PF=0.182$ ).

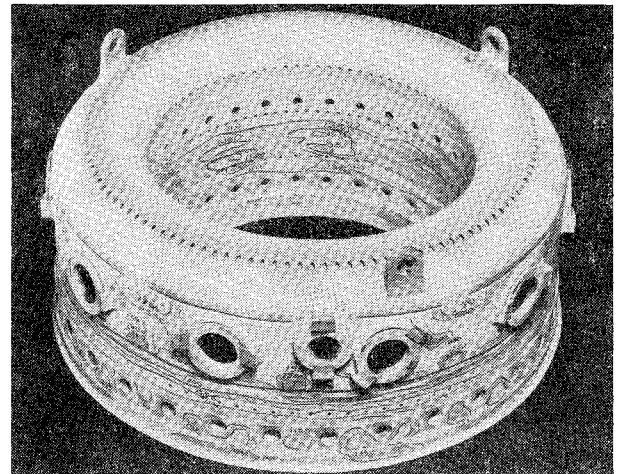


Fig. 5 U.S. Army Concept II liner paint run at sea-level, hot-day maximum power point ( $P_{13}=9.12$  atm,  $T_3=697^\circ\text{F}$  (643 K),  $T_4=2330^\circ\text{F}$  (1550 K),  $\Delta P/P_1=1.9\%$ ,  $PF=0.175$ ).

Table 1 U.S. Army design criteria combustor flow parameters, performance goals, and achieved performance

Performance parameters	Performance goal	Performance achieved	
		Concept I	Concept II
Engine airflow, kg/s	1.302	1.315	1.315
Combustor inlet pressure, MPa	1.01	1.01	1.01
Combustor inlet temperature, K	625	621	625
Combustor exit temperature, K	1533	1539	1528
Combustion efficiency, %			
Idle	98.0	98.08	99.57
Maximum power	99.5	99.99	99.99
Pressure drop $P_{13}$ , %	3.0	2.5	1.7
Pattern factor	0.23	0.17	0.22
Radial pattern factor	0.075	0.014	0.044
Maximum wall temperature, K	1144	1047	1144
Lean blowout, $F/A$	0.004	0.003	0.003
SAE smoke number	34	0	8.5
$\text{NO}_x$ , lb/1000 hp, h, cycle	12.9	5.71	6.92

these combustors used 10 air-assist air-blast nozzles inserted radially through the liner outer wall. The baseline concept I configuration met all of the design objectives over the entire operating envelope from sea level to 20,000 ft altitude (see Table 1). Typical liner wall temperature levels and characteristics, as determined by temperature-sensitive paint (Therminox OG-6), for sea-level, hot-day, maximum conditions are shown in Fig. 4. The maximum temperatures for the outer and inner liner walls were  $1200^\circ\text{F}$  (992 K) and  $1425^\circ\text{F}$  (1047 K), respectively. The liner wall temperature gradients were within the desired  $500^\circ\text{F/in.}$  level. The measured pattern factor was 0.182 at an average discharge temperature of  $2407^\circ\text{F}$  (1593 K) and a combustor total pressure drop of 2.3%.

The basic concept II configuration did not meet the design goals in regard to combustor exit temperature quality, wall temperature levels and gradients, and lean blowout characteristics. At first, it appeared that the model predictions were totally inaccurate. However, upon examination, it was found that the errors were due to improper assumptions in the liner boundary conditions and an inadvertent change in the axial location of the inside diameter primary orifices during the detail design phase. When hardware changes were made to correct these errors, performance of the modified concept II was considerably improved, as summarized in Table 1. It also met all of the design objectives and the liner

wall temperature level and gradients (see Fig. 5) were acceptable for combustor durability.

Extensive use was made of various multidimensional models during the design and testing phase of an annular reverse-flow premix/prevaporizing combustor (concept III).<sup>8</sup> A number of hardware modifications as guided by analysis were investigated to assess the effect of the following on combustor performance and emissions: 1) premix to pilot zone air and fuel flow splits, 2) premix length, 3) pilot nozzle flow number.

The best overall emission reductions for concept III were obtained with 0.9 flow number pilot pressure atomizers and 20.3 cm premix injection length. See Fig. 6. At the simulated takeoff point, the pilot fuel flow rate was 30% of the total and the airflow rate in the premix/prevaporization passage was 24%. The emissions levels (CO, HC, and  $\text{NO}_x$  emission indices) demonstrated by concept III were significantly lower than the production combustor (diffusion flame) configuration, as summarized in Fig. 6. At the takeoff power point, the smoke number was 0, combustion efficiency 99.94%, the pattern factor 0.15, and total pressure drop 4.4%.

An extensive technical effort consisting of detailed analytical modeling, element rig testing, and full-scale rig testing was undertaken to develop an annular reverse-flow ceramic combustor technology base.<sup>3</sup> The main objective of this effort was to significantly reduce liner wall temperature gradients. The required performance and durability objectives were achieved, in addition to verifying the predictions for significant wall temperature gradient reductions as compared with the baseline configuration.

A number of air and/or fuel staging concepts can be applied for increasing operability range of future high-temperature-rise turbopropulsion combustors. A variable geometry (VG) combustor concept (see Fig. 7) was designed and developed with the help of combustor analytical models.<sup>9</sup> This combustor used 20 piloted airblast nozzles inserted axially through the dome. Each fuel nozzle was concentrically surrounded by two corotating axial swirlers. The combustor airflow distribution with VG open was such that the primary zone air amounted to approximately 74% of the total combustor air. To achieve an acceptable primary zone fuel:air ratio at low-power conditions, the amount of dome air was controlled. The combustor lean blowout characteristics were significantly improved compared with the baseline configuration without air and fuel staging (see Fig. 7).

Extensive use of analytical models was also made in a segmented ceramic combustor for the U.S. Air Force Wright

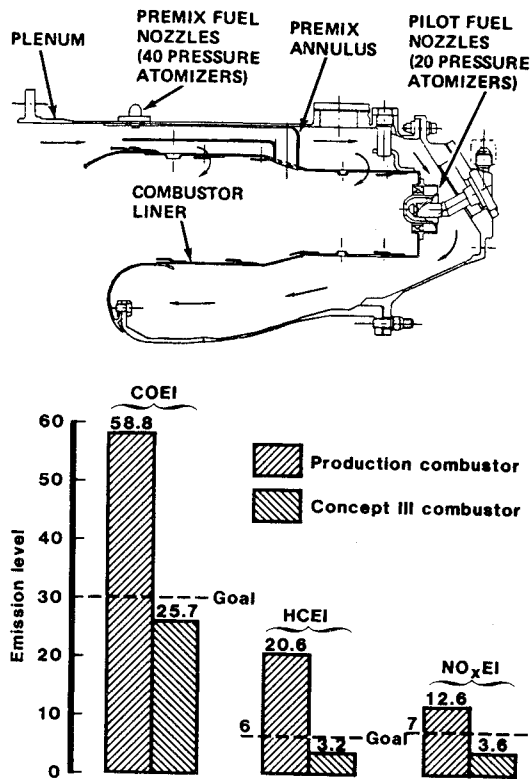


Fig. 6 NASA PRTP concept III combustion and demonstrated emissions levels.

Aeronautical Laboratories (AFWAL).<sup>10</sup> This combustor's final configuration evolved through a number of iterations, where variations in the dome detail design and fuel nozzle characteristics were analytically evaluated to satisfy the conflicting requirements of maintaining low, uniform near-wall gas temperatures and soft light-off to ensure structural durability in addition to other performance parameters of stoichiometric combustors. The basic combustor, as shown in Fig. 8, demonstrated excellent performance in regard to ignition, lean blowout, wall temperature characteristics, pattern factor, and combustion efficiency.<sup>11</sup>

To design a lean-burn, low-emission combustor for a regenerative automotive gas turbine engine application, a number of combustor configurations were analyzed by a two-dimensional elliptic reacting flow model.<sup>12</sup> The analytical investigation consisted of variations in combustor design details, including airflow splits, swirl angle, fuel flow splits, spray quality, and prechamber dimensions. The analytical modeling effort followed by bench-scale testing produced a unique combustor concept with internal flowfield characteristics that allowed internal fuel/air mixing (see Fig. 9) to minimize NO<sub>x</sub> emissions.

In addition to the combustors just discussed, analytical models have been used for a number of other gas turbine combustors. The models have been found to be useful for designing advanced combustors. They have improved insight into solving many engine combustor development problems over the last 10 years. Even though the models have proved useful for combustor design purposes, they have exhibited serious limitations, as will be described in Sec. IV.

#### IV. Assessment and Limitations as a Design Tool

As discussed in Sec. III, a number of gas turbine combustors have been designed over the last 10 years by judiciously using the empirical data base, multidimensional analytical techniques, and test rigs. These combustors have

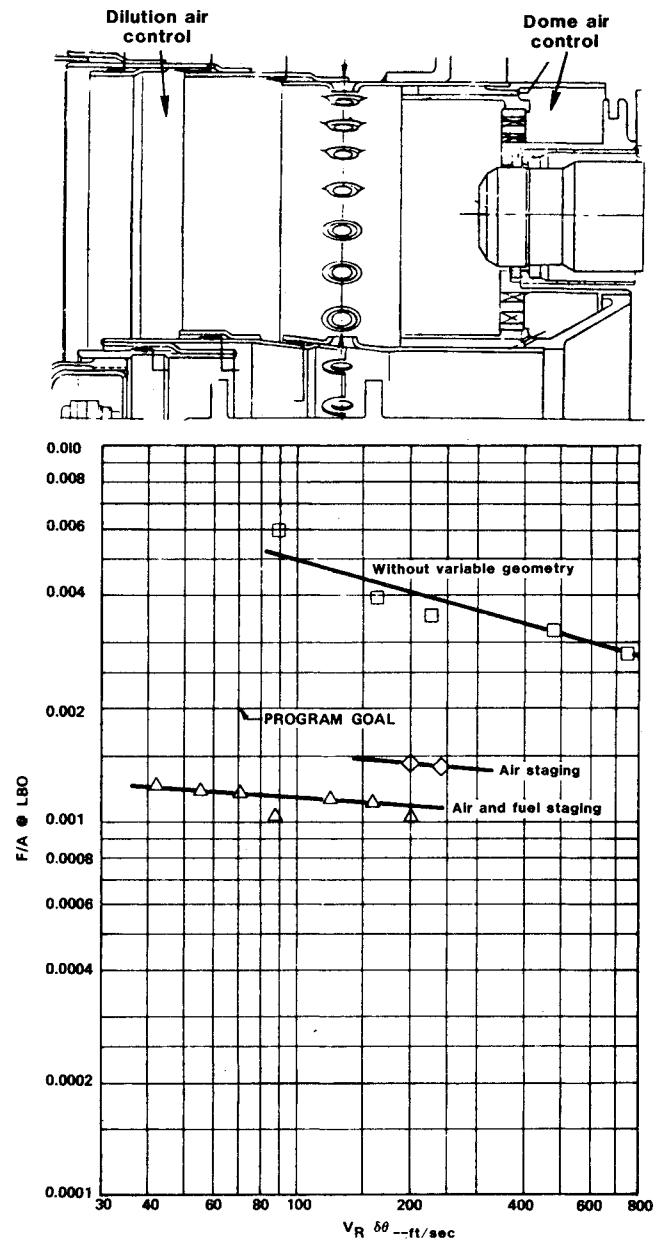
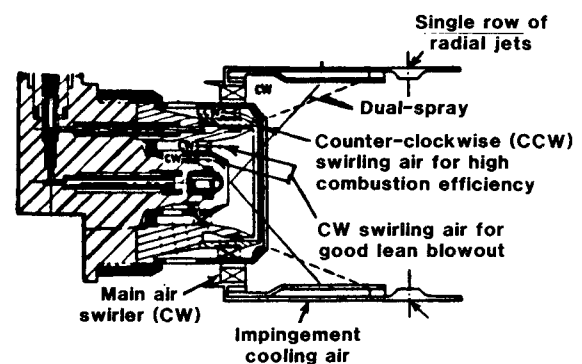


Fig. 7 Variable geometry combustor lean blowout characteristics.



$$P_3 = 150 \text{ lb/in.}^2$$

$$T_4 = 3530^\circ\text{F}$$

$$\text{Combustion efficiency} = 99\%$$

$$\text{Heat release rate} = 13.7 \times 10^6 \text{ Btu/hr-ft}^3$$

$$\text{Sea-level idle lean blowout } f/a = 0.0012$$

$$W_{a3} = 6.6 \text{ lb/sec}$$

$$f/a = 0.053$$

Fig. 8 Segmented ceramic combustor designed with analytical models.<sup>10</sup>

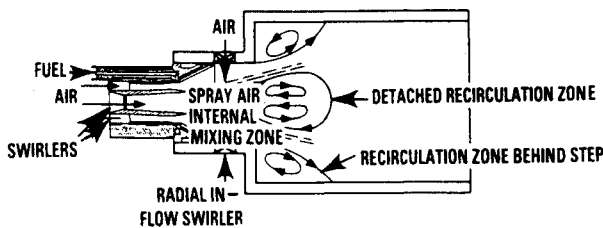


Fig. 9 Internal premix concept for low-emission automotive gas turbine engine application.

demonstrated significant advances in regard to the following parameters:

- 1) Combustor temperature rise.
- 2) Combustor heat release rate.
- 3) Control of wall temperature levels and gradients.
- 4) Lean flame stability and ignition.
- 5) Combustor length and exit temperature quality.
- 6) Gaseous and smoke emissions.

Although the models have been useful during combustor design and development phases, significant advances are needed in the numerics and physical submodels to improve the model's capability to accurately predict complex reacting flows encountered in gas turbine combustors. Starting with the first combustor development, it has been recognized that, to improve model accuracy, updates are needed in the following areas: turbulence and scalar transport models; chemical kinetics; turbulence/chemistry interaction; fuel injection, atomization, spray dynamics, evaporation/combustion, and fuel/air mixing; soot formation/oxidation; and multidimensional radiation modeling.

In addition, one must give consideration to numerical accuracy, mathematical simulation of practical gas turbine combustor hardware, and the boundary condition specification. Some discussion on the numerical accuracy is given in Sec. VI. Body-fitted coordinate systems are slowly being employed for combustor analysis; such systems will provide the needed geometry flexibility.

It is obvious that the boundary conditions must be reasonably known or that there should be a consistent way of estimating them to make meaningful calculations for internal profiles of velocity, species, temperature, and fuel/air ratios. Of primary interest are:

- 1) Combustor airflow distribution, including jet velocities and angles, annulus air velocity, and temperature distribution.
- 2) Cooling airflow distribution, slot gaps, and film velocity when hot.
- 3) Fuel nozzle effective spray angle, droplet size, velocity, and distribution.

Most of these boundary conditions cannot be measured directly; they definitely cannot be evaluated in the real environment. Consequently, they need to be estimated by conducting element tests under controlled conditions and correlated by means of simple models. The models can become quite involved in some cases, e.g., the combustor/diffuser model for through-flow combustion systems. Nevertheless, no matter how much detailed investigation is conducted to establish the boundary and initial conditions for a given combustion system, engineering estimates will have to be made for many other variables in order to simulate the real hardware configuration. In other words, some degree of numerical/experimental iterations need to be made for every combustor analysis. This also applies to the following boundary conditions of secondary importance: 1) turbulence levels and length scales associated with various injection points; 2) velocity and temperature distribution through air injection orifices; 3) details of the cooling slot film; and 4) special treatment required for various disturbances within the flowfield.

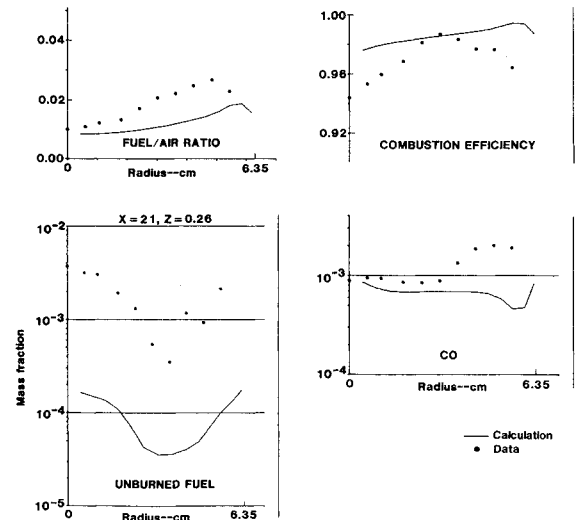


Fig. 10 Typical comparison between data and calculations for the U.S. Army can combustor.<sup>13</sup>

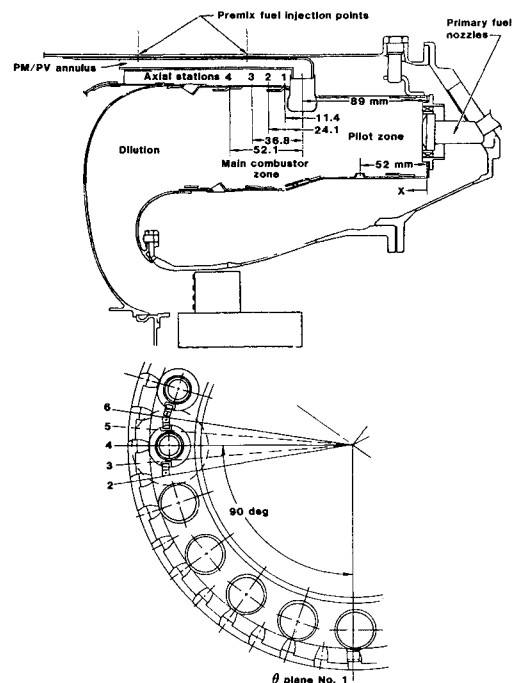


Fig. 11 Annular PM/PV combustor for model validation.<sup>2</sup>

Perhaps the most difficult of all is how to account for the variabilities caused by manufacturing and those associated with engine operation in the field. Consequently, multidimensional models cannot predict the following important design parameters of interest: 1) burner exit pattern factor; 2) hot streaks caused by manufacturing related variations in liner dimensions and fuel nozzle spray characteristics; and 3) combustor lean-flame stability and ignition characteristics. Even though current multidimensional combustion models cannot predict some of the design parameters and have many deficiencies, their usefulness as design guides is well established (see Sec. III). To assess their limitations, detailed internal flow mapping and model calculations have been done on a number of gas turbine combustors. Typical comparisons for some of these combustors are presented in the following paragraphs.

An extensive amount of model validation was conducted under an Army-sponsored program.<sup>13</sup> The test rigs used in this investigation included liner cooling, jet mixing, and can

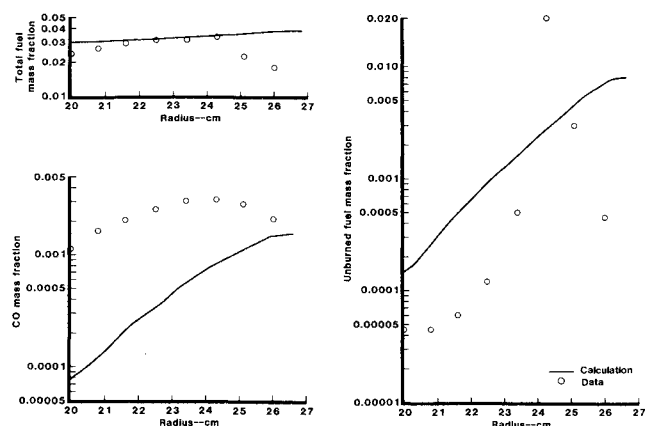


Fig. 12 Typical comparison between predictions and data at  $x=1$  and  $\theta=3$  station.

combustor. Radial profiles of CO, CO<sub>2</sub>, NO<sub>x</sub>, and unburned hydrocarbons were measured at different axial locations of a 12.7 cm diam can combustor. The mapping was conducted with both gaseous (natural gas) and liquid (Jet-A) fuels. A water/steam cooled stainless steel emission probe with 10 individual sampling ports was used. The radial profiles were measured at up to eight axial stations (some of which were within the primary zone) and five circumferential locations. A total of 13 sets of data were taken over the following range: pressure = 2-10 atm,  $T_3 = 370$ -620 K, combustor pressure drop = 3-10%, and fuel:air ratio = 0.006-0.015.

A three-dimensional elliptic code with  $k$ - $\epsilon$  model of turbulence, a two-step kinetic scheme with modified eddy breakup model, was used to correlate the measured data. A 60 deg sector of the combustor was divided into  $32 \times 16 \times 14$  finite difference nodes along axial, radial, and circumferential directions, respectively. Figure 10 shows a typical comparison between the data and prediction for an axial station that is 21 cm from the nozzle face. The fuel:air ratio profile comparison is reasonable, but more needs to be done to claim good agreement for unburned hydrocarbons, CO, and combustion efficiency.

To assess the model accuracy for annular combustors, a premix/prevaporizing combustor (see Fig. 11) was mapped.<sup>2</sup> The radial profiles of CO, CO<sub>2</sub>, unburned hydrocarbons, and NO<sub>x</sub> were measured at four axial stations and six circumferential  $\theta$  planes within the main combustion zone. A water/steam-cooled probe was used to obtain the radial profiles. The internal emission mapping at 1 atm was conducted to parametrically investigate the effect of combustor inlet temperature, overall fuel:air ratio, and fuel-flow splits between the pilot and main combustion zone on the emission profile. The three-dimensional code was used for validation purposes. Typical results are shown in Figs. 12 and 13 for two stations, namely, 1)  $x=1$  and  $\theta=3$  and 2)  $x=2$  and  $\theta=4$ . As shown, the agreement is reasonable for fuel:air ratio profiles. However, the comparison for CO and unburned hydrocarbons is not good. This is consistent with what was seen in the U.S. Army can combustor data validation discussed previously.

Model validation was recently conducted for a low-emission can combustor on an element test rig.<sup>12</sup> The test results were obtained for both nonreacting and reacting flows. A two-beam, back-scattering laser Doppler velocimeter (LDV) system was used for measuring the velocity profiles in the nonreacting environment. A single-point emission probe was used to measure CO<sub>2</sub> concentration for investigating the mixedness. Typical results are presented in Fig. 14, where it can be seen that predictions qualitatively agree with the data, but that the quantitative agreement is

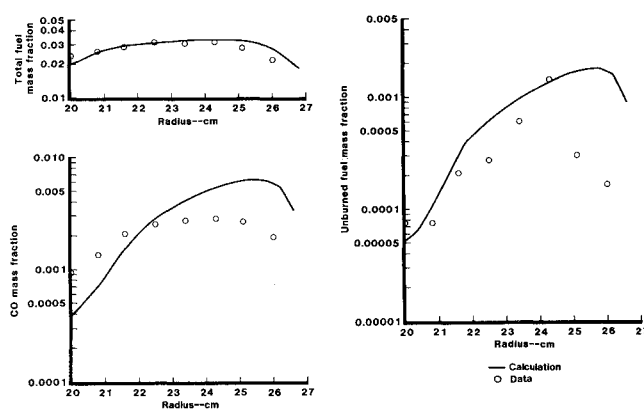


Fig. 13 Typical comparison between predictions and data at  $x=2$  and  $\theta=4$  station.

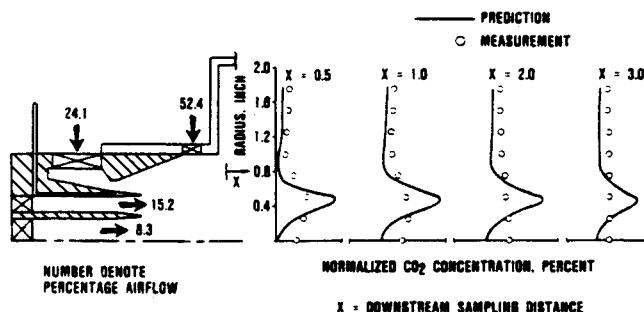


Fig. 14 Typical comparison between predicted and measured CO<sub>2</sub> concentration in a nonreacting low-emission combustor element test.<sup>12</sup>

poor. Similar conclusions can be reached for the reacting flow data, as shown in Fig. 15.

Based on results on previously mentioned combustors and limited comparisons of other, it can be concluded that current multidimensional combustion models provide qualitatively good comparison with measurements. Therefore, they can be used as an adjunct to an empirical design approach to provide better insight into the various physicochemical processes occurring within gas turbine combustors. As physical submodels and numerics accuracy improve, analytical models will play a vital role in the design and development process. In spite of the many deficiencies in the current models, they have been found useful for making relative comparisons between different design changes so that only a few promising concepts need to be designed, fabricated, and tested instead of a purely empirical-based approach with the attendant large number of hardware modifications.

## V. Assessment of Physical Models of Turbulent Reactive Flows

Gas turbine combustion models include submodels of turbulence, chemical kinetics, turbulence/chemistry interaction, spray dynamics, evaporation/combustion, radiation, and soot formation and oxidation. A number of researchers are involved in the formulation and validation of these models. A brief overview of the work will be presented. The majority of the validation effort has been for the assessment of the following models:

- 1) Two-equation ( $k$ - $\epsilon$ ) turbulence model and its modifications to account for the low Reynolds number flow (in wall shear flows), streamline curvature, and swirl.
- 2) Algebraic stress model for parabolic flow and limited attempt for elliptic flows.

- 3) Two- and four-step global kinetic schemes for predicting hydrocarbon combustion rates.
- 4) Semiglobal reaction schemes for predicting  $\text{NO}_x$ .
- 5) Modified eddy breakup model.
- 6) Spray dynamics, evaporation, and combustion.

A limited amount of work has been done in validating radiation models and soot formation and oxidation modeling.

An extensive amount of model validation was conducted under an Army-sponsored program.<sup>13</sup> The following element test rigs were used in this investigation: liner cooling, jet mixing, can combustor, and combustor transition liner mixing.

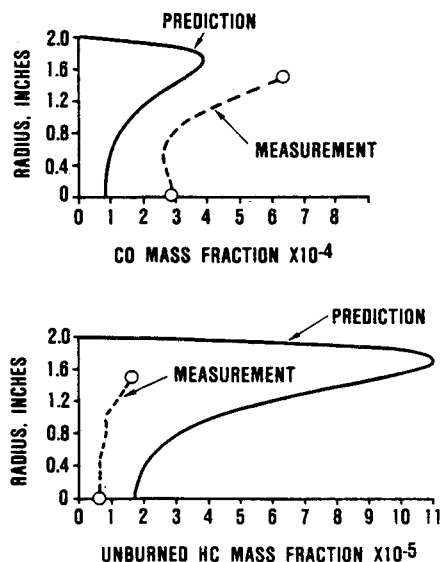


Fig. 15 Reacting flow test data and predictions for the low-emission combustor element.<sup>12</sup>

Subsequent model validation has continued under three NASA-sponsored programs.<sup>14-16</sup> The work presented in Ref. 14 will be described briefly in the following paragraphs.

Over the years, a number of test cases have been computed. These flows can be broadly divided into the following three categories: 1) simple flows with no streamline curvature, 2) complex flows without swirl, and 3) complex flows with swirl.

A partial list of test cases from each of these categories is presented in Figs. 16-18. A total of 13 test cases of simple flows have been calculated by using a GENMIX-based parabolic program.<sup>17</sup> For all these cases, the measured profiles (when available) of mean and fluctuating variables were used at the initial station. One hundred nonuniformly spaced grid points were used in these computations. Predictions were compared with data of Watts and Brundrett,<sup>18</sup> Emery and Gessner,<sup>19</sup> El Telbany and Reynolds,<sup>20</sup> Barbin and Jones,<sup>21</sup> Laufer,<sup>22</sup> Saiy and Peerless,<sup>23</sup> Champagne and Wygnanski,<sup>24</sup> Wygnanski and Fielder,<sup>25</sup> Charnay et al.,<sup>26</sup> Hartman et al.,<sup>27</sup> and Hassan and Lockwood.<sup>30</sup>

For assessing the model accuracy in complex nonswirling flows, calculations were performed for a total of 10 test rigs, as shown in Fig. 17. The two-dimensional parabolic code was used for the Shivaprasad test setup.<sup>31</sup> For other cases, the two-dimensional elliptic code was used. Typically, 2000 finite difference nodes were employed in these calculations. The numerical convergence was checked by comparing variations in the following parameters:

- 1) Maximum local mass continuity residual ( $R_{\max}$ ) normalized by inlet flow rate.
- 2) Cumulative mass continuity residual ( $R_{\text{sum}}$ ) normalized by inlet mass flow rate.
- 3) Variations in the dependent variables from iteration-to-iteration ( $\Delta\phi$ ) normalized by the inlet value.

Typically, 400 iterations were required to achieve the following levels:  $R_{\max} = 0(10^{-5})$ ,  $R_{\text{sum}} \leq 0.001$ , and  $\Delta U = 0(10^{-4})$ .

The two-dimensional elliptic predictions were compared with data of Kim et al.,<sup>32</sup> Eaton and Johnston,<sup>33</sup> Phataraphruk and Logan,<sup>34</sup> Moon and Rudinger,<sup>35</sup> Fujii,<sup>36</sup> Lightman et al.,<sup>37</sup>

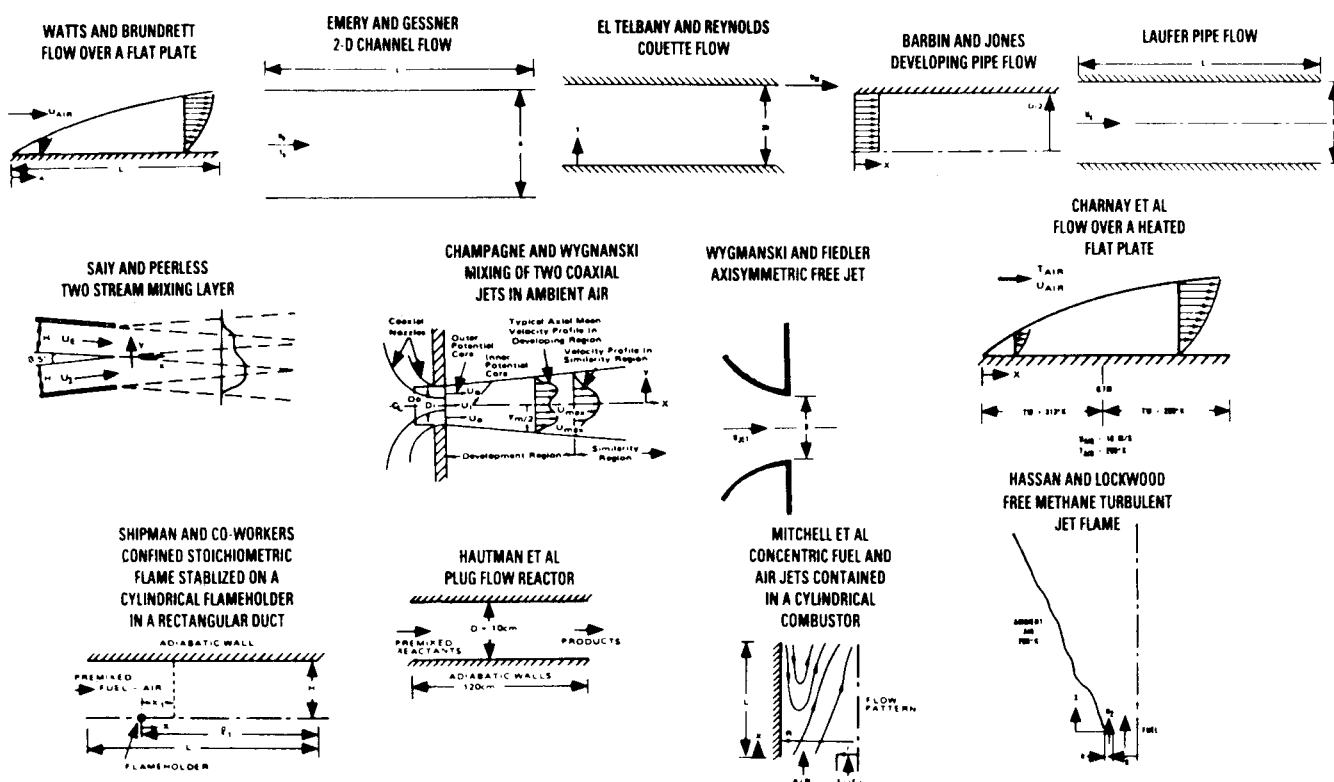


Fig. 16 List of computed simple flows.<sup>14</sup>

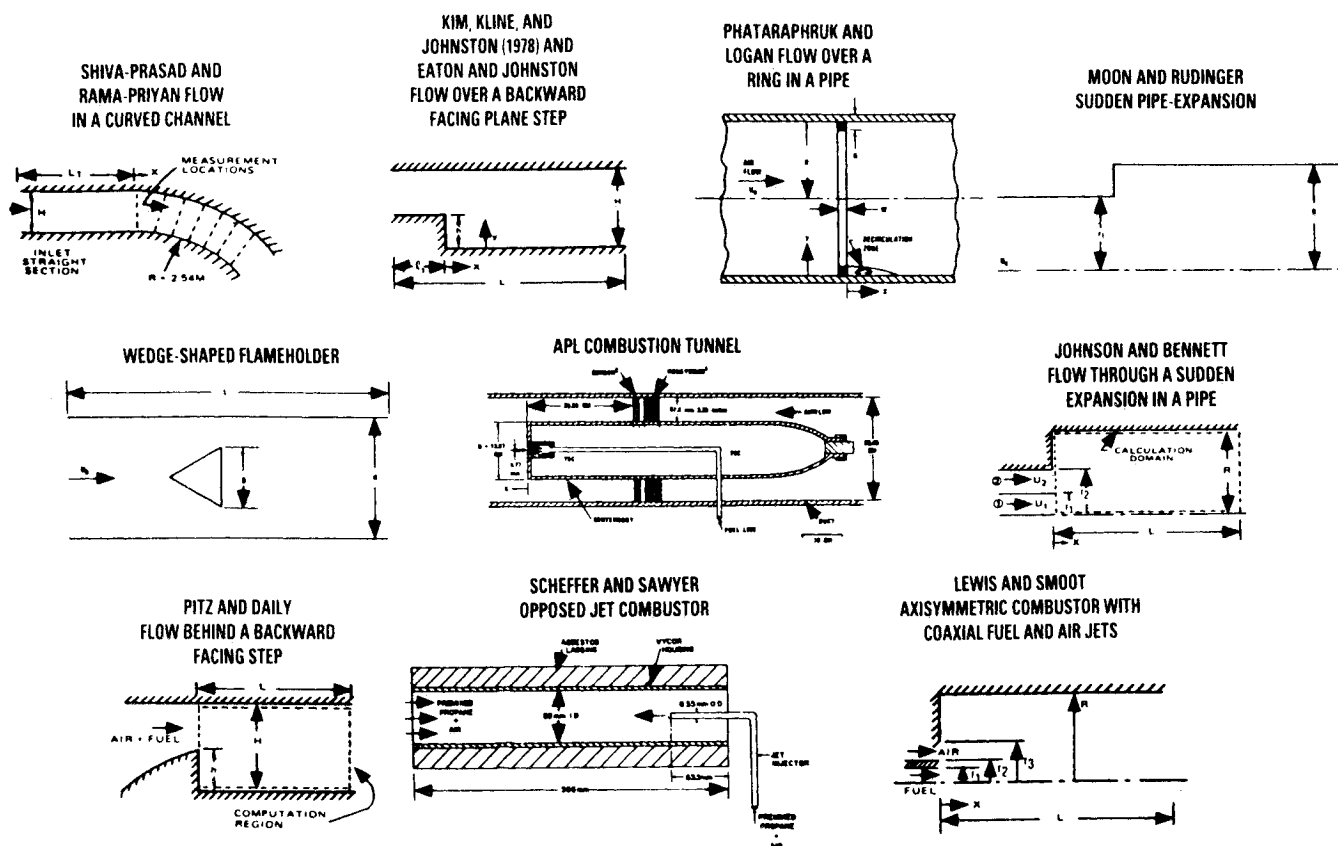


Fig. 17 List of complex nonswirling flows computed in Ref. 14.

Johnson and Bennett,<sup>38</sup> Pitz and Daily,<sup>39</sup> Schefer and Sawyer,<sup>40</sup> and Lewis and Smoot.<sup>41</sup> The results for all these cases are presented in Ref. 14.

Model predictions have been compared with swirling flow data of Morse,<sup>42</sup> GTEC,<sup>43,44</sup> Brum and Samuelsen,<sup>45</sup> Lilley and associates,<sup>46</sup> Jones and associates,<sup>47</sup> and El-Banhawy and Whitelaw.<sup>48</sup> Detail discussion for all these cases is given in Ref. 14.

General assessment for an extensive investigation spanning a period of 10 years can be made in a number of ways. Here the assessment is made for each of the major submodels and what their capabilities are in predicting various types of flows: simple, complex nonswirling, and swirling flows. In the following paragraphs, statements are frequently made regarding a model giving good results, reasonable results, trends, or unsatisfactory results. This implies the following: a model is termed good when it can correlate data within  $\pm 25\%$ . A reasonable correlation implies agreement within a factor of 2.0. When a model is called qualitatively good or is described as predicting trends, no claim is made in regard to quantitative accuracy of this model. Predictions of such a model when used in a combustor design system should be cautiously interpreted for guiding an engineering design.

#### $k-\epsilon$ Turbulence Model

This includes the standard  $k-\epsilon$  model of turbulence and its various modifications, including corrections for the low Reynolds number, additional strain due to streamline curvature and swirl (Richardson number correction), and other ad hoc assumptions for changing empirical constants  $C_D$ ,  $C_2$ , and Prandtl/Schmidt numbers. The following general conclusions are made regarding the  $k-\epsilon$  model capabilities:

- 1) Gives good correlation for simple flows.
- 2) Requires low Reynolds number correlation for predicting wall shear layers.
- 3) Requires different model modifications for accurately predicting curved (convex and concave) boundary layers.

4) Gives good correlation for the far-field regimes of complex swirling or nonswirling flows involving regions of recirculation.

5) Gives reasonable results for nonswirling recirculating flows. (The correlation is not as good in the vicinity of reattachment points.)

6) Gives reasonable correlation for confined disk flow with jet at the center.

7) Gives good correlation for nonrecirculating swirling flows.

8) Predicts outer regions of strong swirling flows well. (A reasonable correlation is achieved for the shear layer between the outer region and the recirculation zone. Trends are properly predicted for the recirculating flow regions.)

9) Gives reasonable correlation for most of the flow region established by a confined swirler, with expansions on both hub and shroud sides.

10) Predicts trends for confined swirler with no outer expansion.

#### Algebraic Stress Model and Its Modifications

This model predicts mean flowfield properties as well as the  $k-\epsilon$  model does. Therefore, the comments in the previous paragraph apply to the algebraic stress model (ASM) as far as the mean velocity field is concerned. The following conclusions are made in regard to the Reynolds stresses for both normal and shear stress components:

- 1) All Reynolds stress components are predicted reasonably well for simple flows.
- 2) A low Reynolds number correction is required for predicting wall shear layers.
- 3) Different modifications are required for predicting convex and concave wall shear flows.

#### Scale Transport Model

The  $k-\epsilon$  model with specified Prandtl number predicts scalar fluxes reasonably well for the flows where gradient



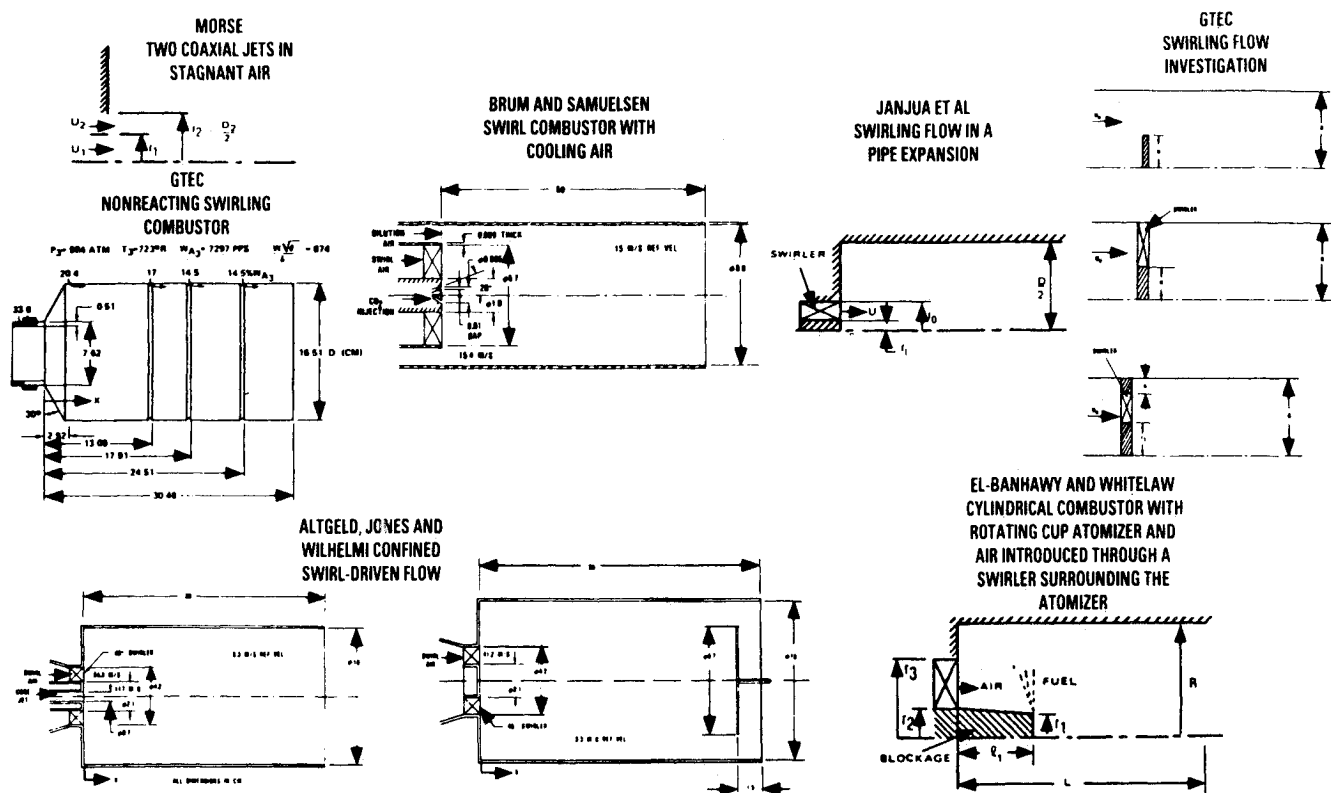
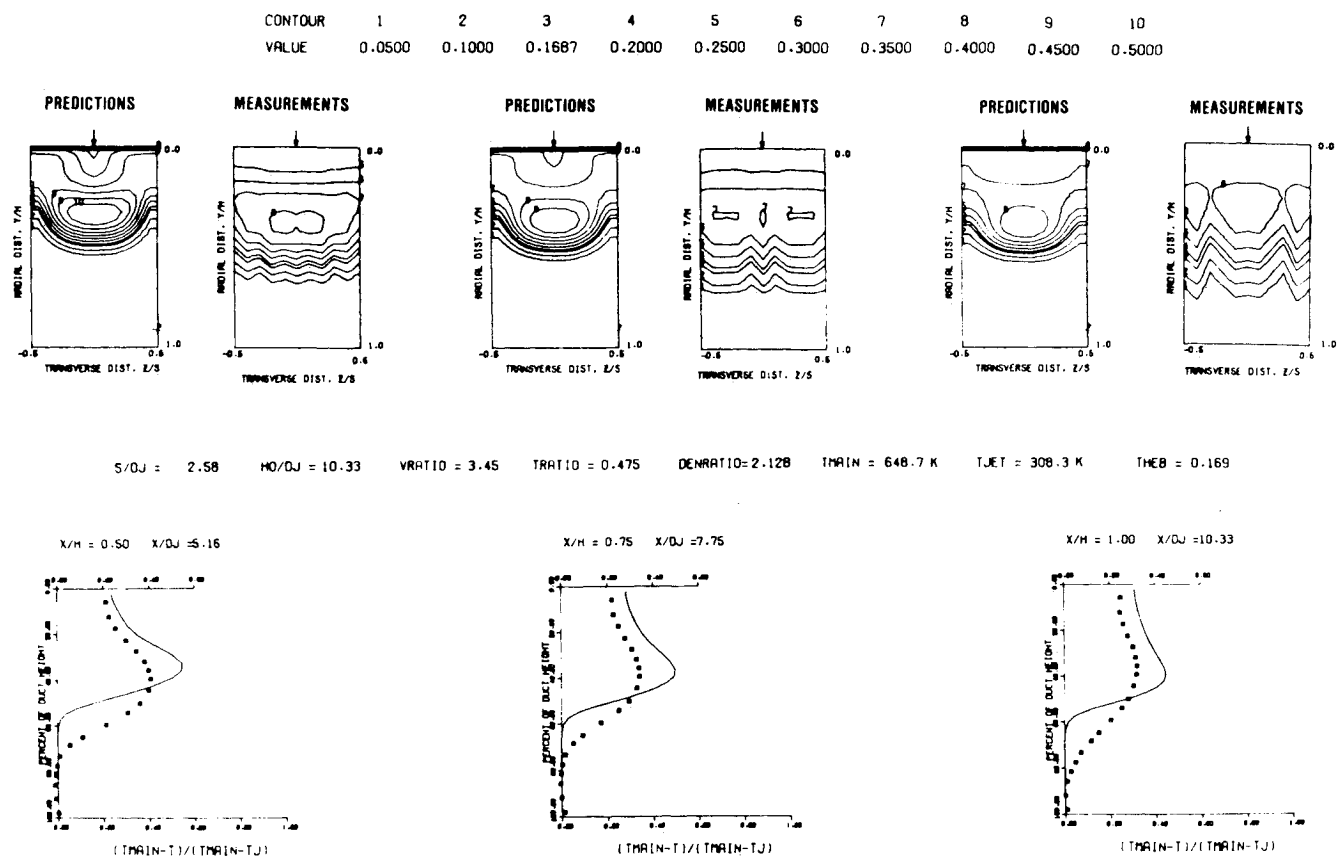


Fig. 18 List of swirling flows reported in Ref. 14.

Fig. 19 Comparison between data and predictions for test 1 (straight duct,  $TM = \text{const}$ ,  $J = 25.32$ ,  $S/D = 2.00$ ,  $H/D = 8.00$ , number of nodes = 19,890).

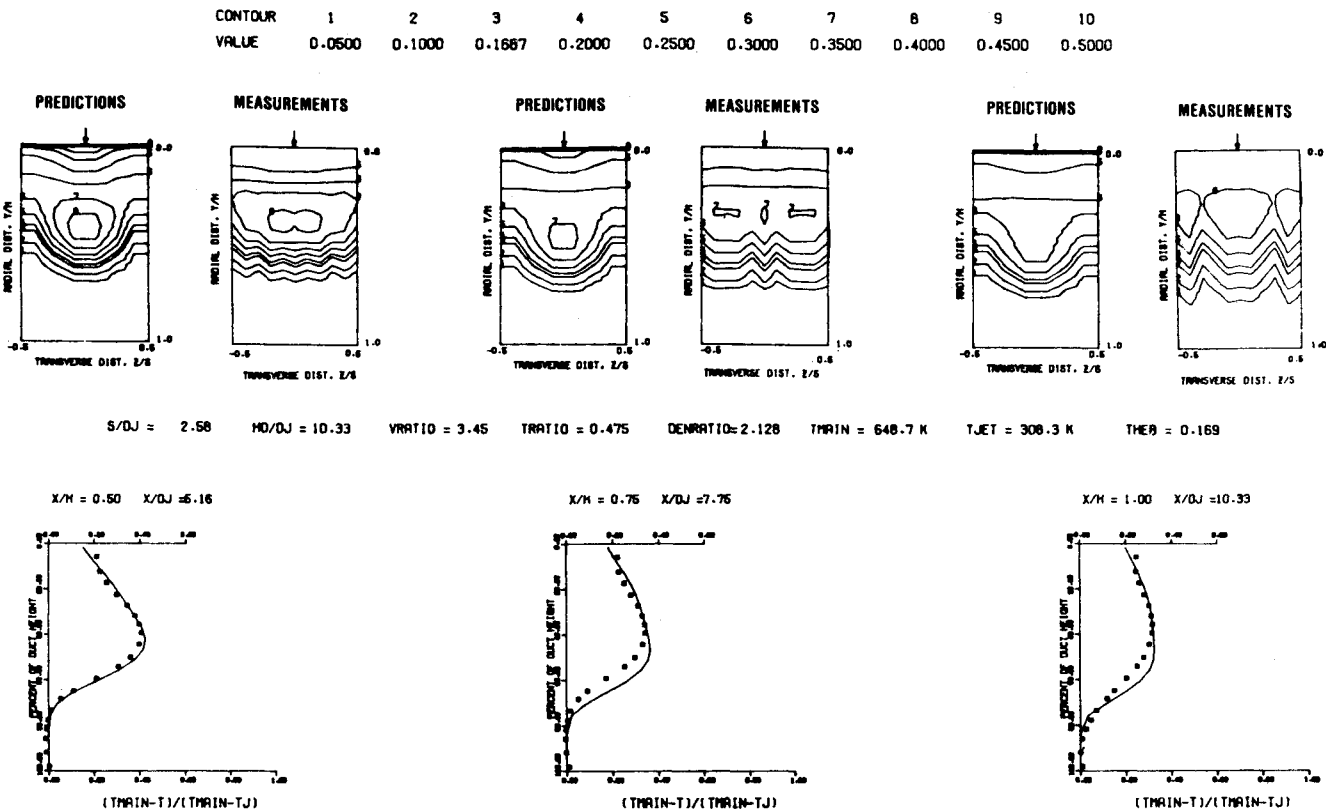


Fig. 20 Comparison between data and predictions for test 1 (straight duct, four-node jet,  $J=25.32$ ,  $S/D=2.00$ ,  $H/D=8.00$ , number of nodes = 5615).

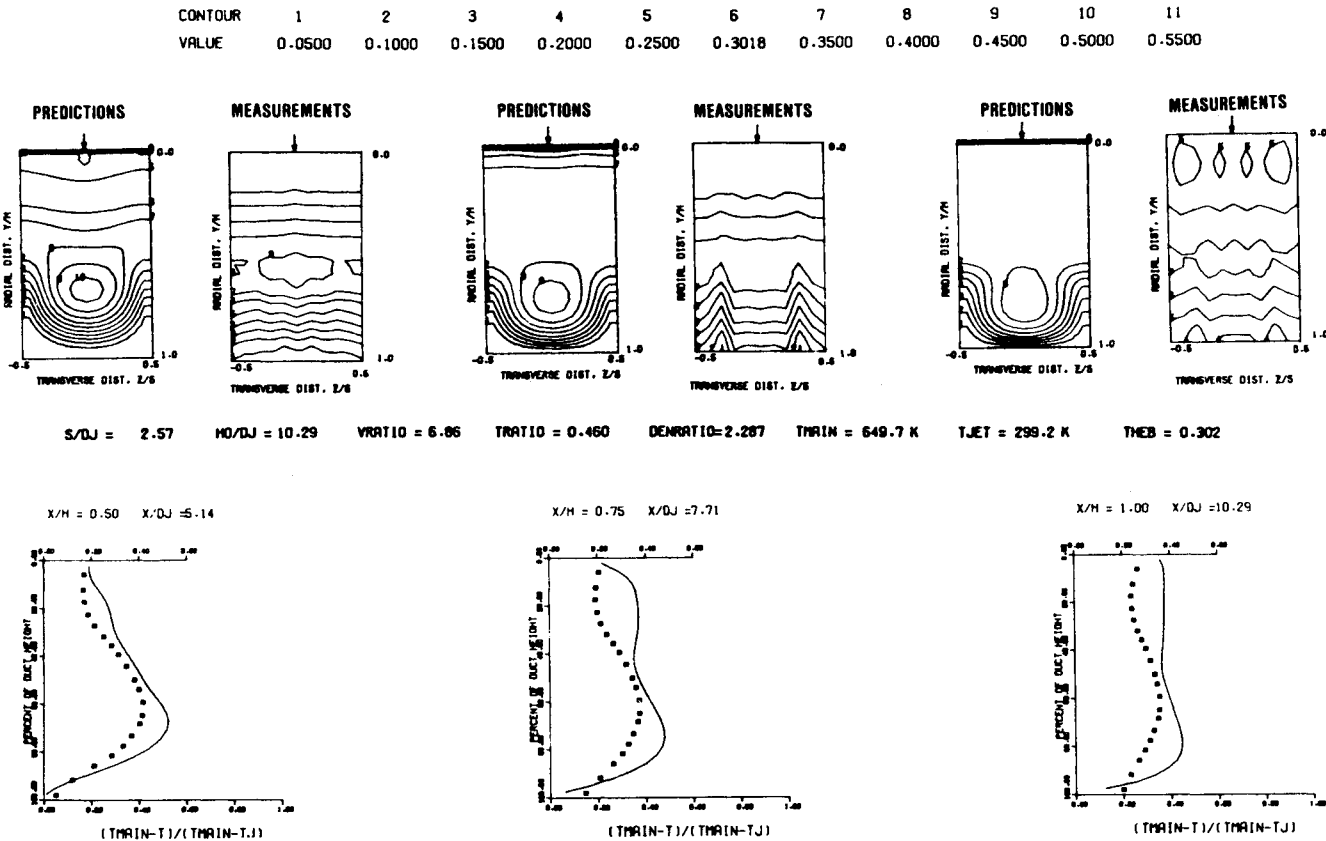


Fig. 21 Comparison between data and predictions for test 6 (test section 1,  $TM=const$ ,  $J=107.78$ ,  $S/D=2.00$ ,  $H/D=8.00$ , number of nodes = 19,690).

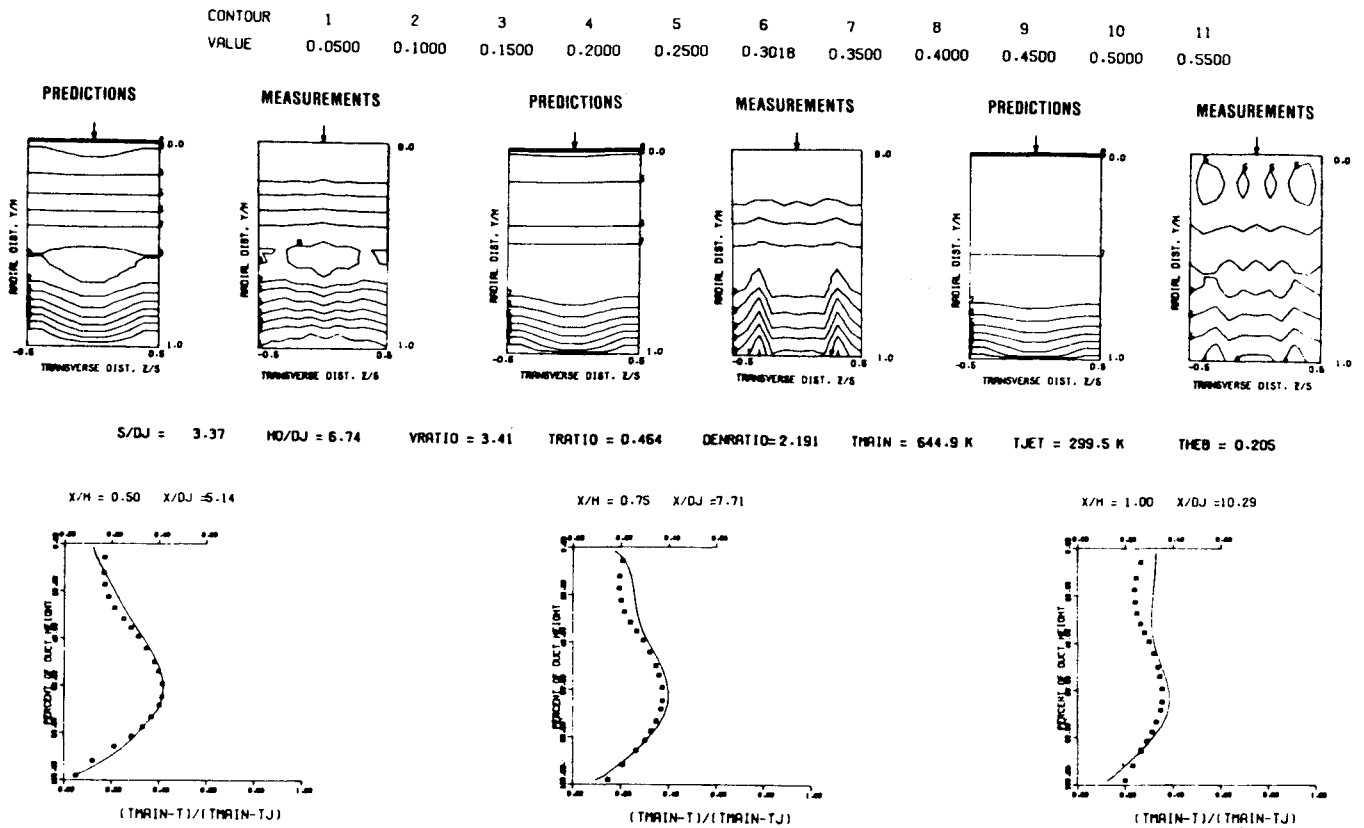


Fig. 22 Comparison between data and predictions for test 6 (straight duct, four-node jet,  $J=107.78$ ,  $S/D=2.00$ ,  $H/D=8.00$ , number of nodes = 5616).

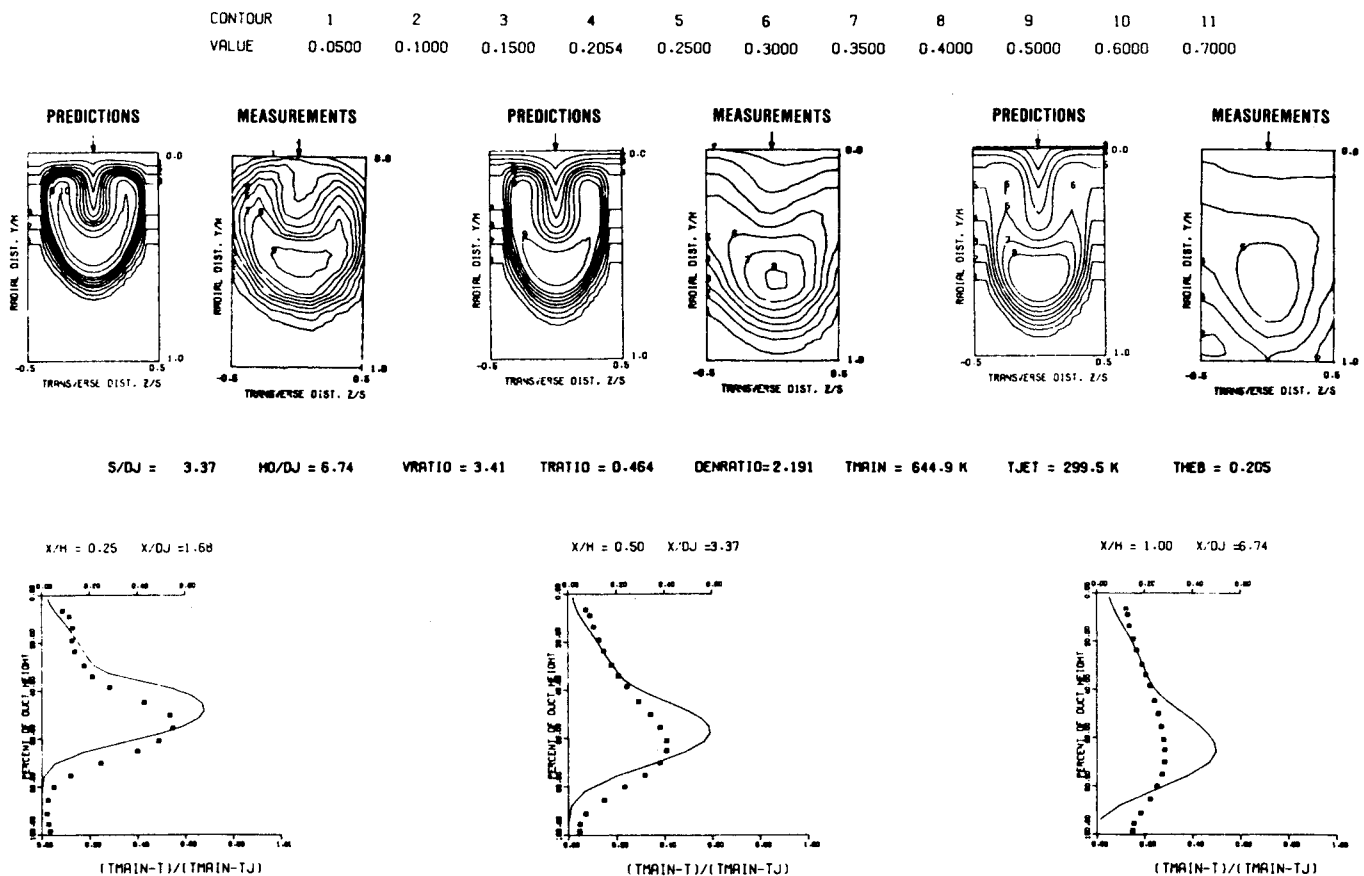


Fig. 23 Comparison between data and predictions for  $J=25.48$ ,  $S/D=2.83$ ,  $H/D=5.66$ , using  $35 \times 33 \times 17$  nodes.

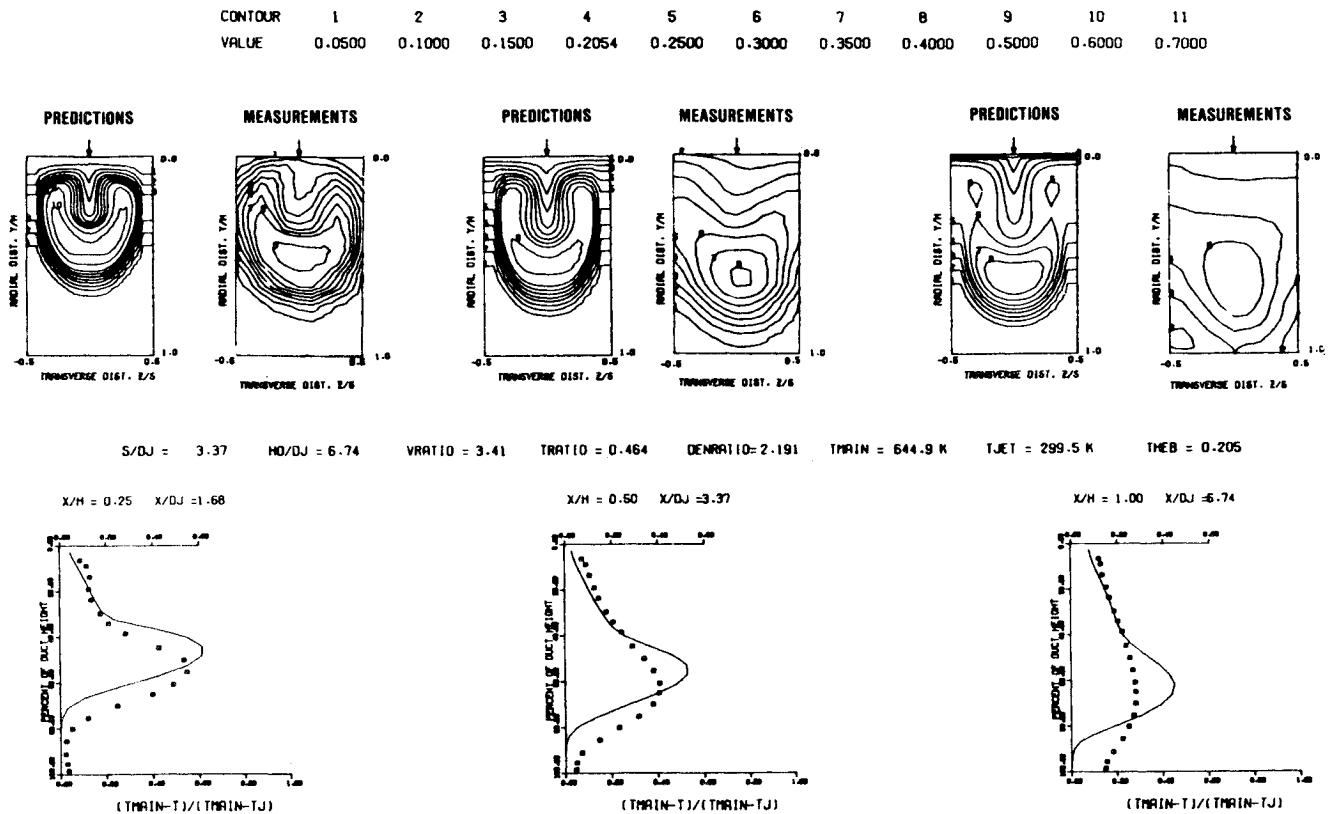


Fig. 24 Comparison between data and predictions for  $J = 25.48$ ,  $S/D = 2.83$ ,  $H/D = 5.66$ , using  $32 \times 29 \times 21$  nodes.

diffusion approximation is valid. The algebraic scalar transport model investigated in Ref. 14 has shown advantages over the  $k-\epsilon$  modeling approach. Further work is needed to establish its validity for recirculating swirling flows.

#### Turbulence/Chemistry Interaction Models

Both two- and four-step reaction schemes show promise for application in gas turbine combustors. They need to be further validated with simple flames (plug flow reactor, diffusion and premixed laminar, and turbulent jet flames) to establish rate constants so that major species including unburned fuel, CO, and  $H_2$  can be accurately predicted.

The modified eddy breakup model predicts trends and should be pursued because this can be easily extended to multistep kinetic schemes, unlike other more vigorous approaches.

A number of points need to be raised here with regard to submodel accuracy. Current state-of-the-art models need to be further developed and verified since they offer many advantages, not least of which are simplicity and an extensive experience data base. However, to sort out various issues, one needs a good set of benchmark quality data for the flows of interest in gas turbine combustors. In addition, the numerical accuracy issue must be resolved before undertaking any future model validation effort.

## VI. Numerical Accuracy

The accuracy of the numerical solution obtained for any given flow problem depends upon the grid density and distribution. One of the parameters frequently used to describe the accuracy of the numerical scheme is the cumulative mass source error. In all the calculations reported in this paper, the cumulative mass source error was less than 0.1% of the total mass flow rate. However, this does not provide any estimate of the numerical diffusion in the finite difference scheme. A procedure for estimating numerical diffusion in the upwind difference scheme has been developed

by McGuirk et al.<sup>49</sup> In their procedure, the local numerical diffusion error is estimated by using the difference between the upwind and central differencing expression for convective terms. By using selective grid refinement, this error is minimized.

The need for an improved numerical scheme is demonstrated in the dilution jet mixing calculations. As a part of the NASA Aerothermal Modeling Program, three-dimensional flowfield calculations were made for the dilution jet mixing problem, using a three-dimensional elliptic code with standard  $k-\epsilon$  turbulence model.<sup>14</sup> The predictions were compared with measurements made under the NASA-sponsored dilution jet mixing program.<sup>50</sup> One of the test cases selected consisted of a row of 12 jets (1.27 cm diameter) injected into a 10.16 cm high duct, having a jet-to-cross-flow momentum ratio of 25.32. The momentum ratio is defined as

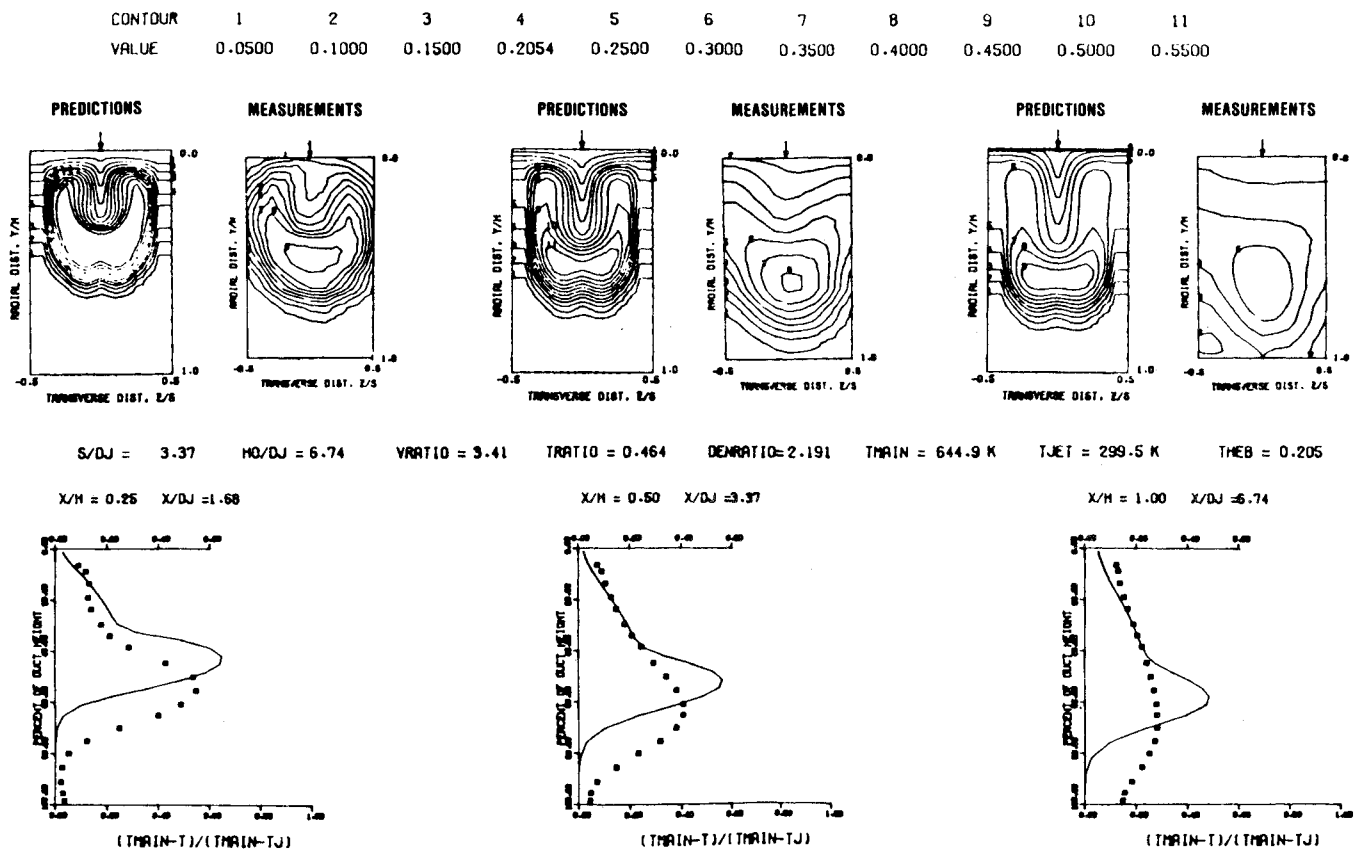
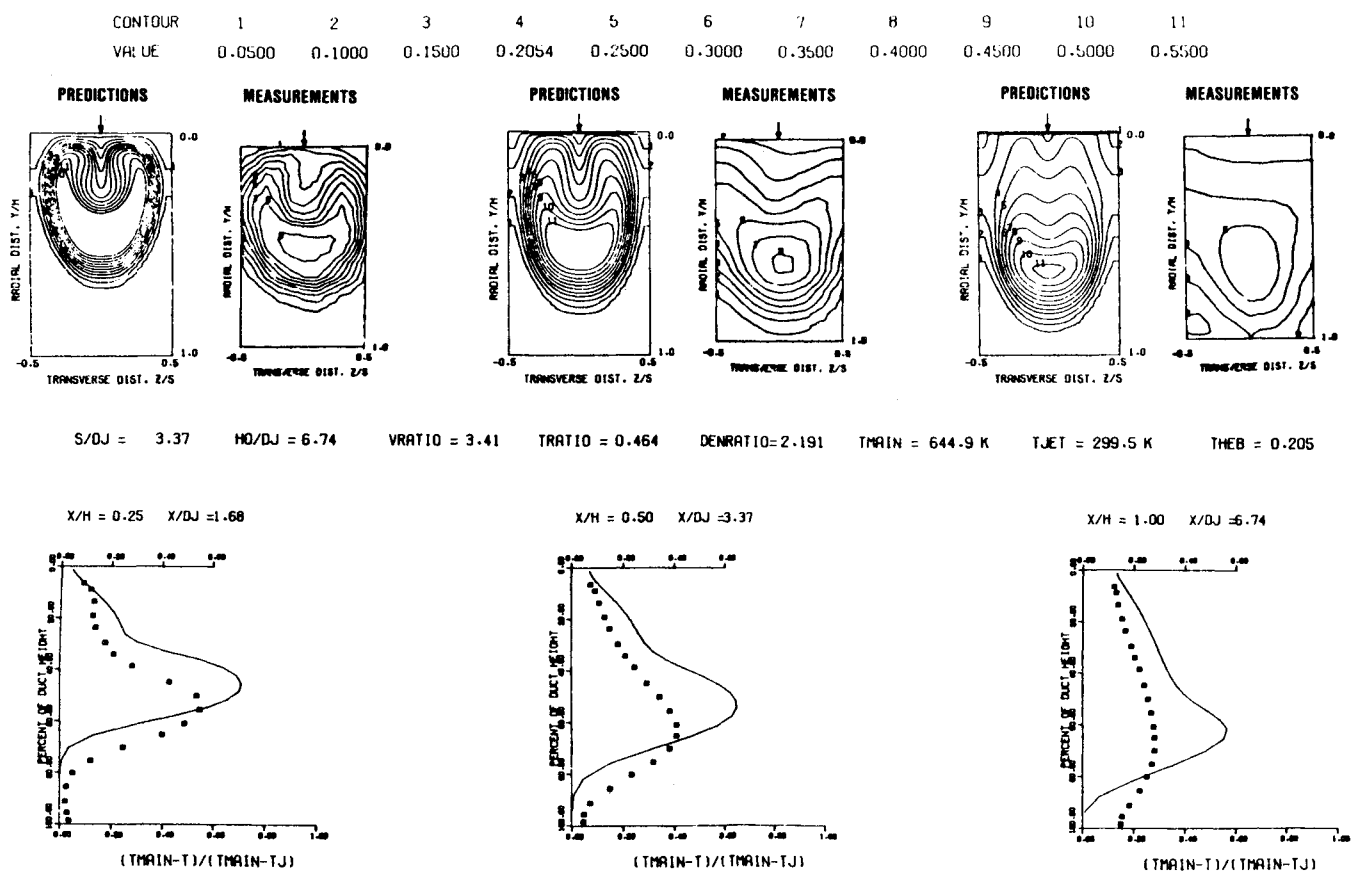
$$J = \rho_j V_j^2 / \rho_m U_m^2$$

The orifice spacing-to-diameter ratio for this case was 2.0. Computations for this case were made by using  $45 \times 26 \times 17$  (19,890) grid nodes in the axial, transverse, and radial directions, respectively. In this case, a total of 49 nodal points were used to simulate each of the radial jets. The predicted temperature distributions were nondimensionalized by using the variable  $\theta$  defined as

$$\theta = (T_m - T) / (T_m - T_j)$$

The comparison between predicted and measured theta distributions is shown in Fig. 19. The predictions shown in this figure are converged results with the total mass source error of about 0.02% of total mass flow rate after 350 iterations. The predicted jet penetrations and mixing rates are slower than those of data.

In most gas turbine combustor flow calculations, it is not possible to have as many as 49 points to simulate a jet. In practice, a maximum of four nodal points are used for

Fig. 25 Comparison between data and predictions for  $J=25.48$ ,  $S/D=2.83$ ,  $H/D=5.66$ , using  $35 \times 33 \times 10$  nodes in half jets.Fig. 26 Comparison between data and predictions for  $J=25.48$ ,  $S/D=2.83$ ,  $H/D=5.66$ , using  $35 \times 33 \times 16$  nodes in half jet.

simulating the jet. To determine the accuracy of the predictions in such cases, calculations were made with a total of  $27 \times 26 \times 8$  (5615) nodal points, of which four nodes were used to simulate the jet. The predicted results for this grid system are shown in Fig. 20. The coarse grid predictions are in much better agreement with the data.

To ascertain that this is not a characteristic of the flow rates, the two grid systems (fine and coarse) were used to obtain predictions for a higher momentum ratio of 107.8. The predicted results for the fine grid system (19,690 nodes) are shown in Fig. 21 and the corresponding results for the coarse grid system (5616 nodes) in Fig. 22. These figures also show that the coarse grid system gives a better correlation with the data than the fine grid network. These results clearly demonstrate that the predictions are not grid-independent solutions.

To determine the effects of grid density, computations were performed with two different grid networks for the case of a single row of 1.8 cm diam jets spaced 5.08 cm apart and having a ratio of jet to cross-flow momentum of 25.48. In one case, a grid network with  $35 \times 33 \times 17$  nodes having 51 nodal points was used to simulate the jets. The predicted results for this case are shown in Fig. 23. The predicted results with this grid system underestimate the jet penetration and the jet spreading rates. The second grid network used for computing this case consisted of  $32 \times 29 \times 21$  nodal points, of which 69 nodes were used to simulate the jets. The predicted temperature field with the second grid system is illustrated in Fig. 24. These results, shown in Figs. 23 and 24, were converged solutions with a total mass source error of 0.02%. The results obtained from the second grid network show a slight improvement in the correlation with the data, especially in the centerplane profiles. Further details of these computations are given in Ref. 14.

The differences in the grid density used for obtaining the results shown in Figs. 23 and 24 are small. To address the effects of the grid density more clearly, two more calculations were made. In these calculations, the computational domain was confined to the region between the jet centerline and the midplane between jets. One of these calculations used a grid network with  $35 \times 33 \times 10$  nodes, of which 45 nodes were used to simulate the jets. The predicted temperature field for this case is shown in Fig. 25. In obtaining the plots, symmetry about the jet centerline was invoked. In the second set of calculations, a total of  $35 \times 33 \times 16$  nodal points were employed, of which 72 nodes were used to simulate the jet. The predicted results for these calculations are shown in Fig. 26. A comparison of Figs. 25 and 26 shows that, by increasing the grid density, an improvement in the jet penetration is obtained; also, the predicted jet spreading rate becomes faster.

The overall conclusion that can be drawn from three-dimensional computations such as jet mixing is that a significantly improved numerical scheme is needed for complex flow computations before various emerging physical submodels of multidimensional turbulent reactive flows can be assessed.

## VII. Summary and Recommendations

Over the last 10 years, an extensive effort has been expanded in the development, validation, and application of multidimensional calculation techniques to augment empirical design procedures. By judiciously combining an empirical data base, engineering judgment, careful interpretation of predictions, and a well-balanced experimental program, it can be concluded that a significantly improved combustor design procedure has evolved. Its further enhancement is predicted on accomplishing the following.

Due to numerical diffusions involved in analyzing recirculating flows, it has been difficult to assess the model accuracy in predicting such flows. Therefore, it is considered

vital to develop a numerical scheme with a higher order of accuracy to minimize the numerical errors.

During the course of the present investigation, it was recognized in many instances that there was a lack of a benchmark quality data base relevant to gas turbine combustion. Such a data base is badly needed for making further modal assessment.

Although the current submodels of turbulent reactive flows do a reasonable job for providing trends, much more needs to be done to improve confidence in the predictive capabilities of multidimensional calculation procedures.

## References

- <sup>1</sup>Mongia, H. C. and Smith, K. F., "An Empirical/Analytical Design Methodology for Gas Turbine Combustor," AIAA Paper 78-998, 1978.
- <sup>2</sup>Reynolds, R. S., Kuhn, T. E., and Mongia, H. C., "An Advanced Combustor Analytical Design Procedure and its Application in the Design and Development Testing of a Premix/Prevaporized Combustion System," paper presented at Spring Technical Meeting, Central States Section of The Combustion Institute, Cleveland, March 1977.
- <sup>3</sup>Johansen, K. M., Johnston, B. H., Mongia, H. C., and Sanborn, J. W., "Combustion Process Testing for Reduced Wall-Temperature Gradients," *Proceedings, DARPA/NAVSEA Ceramic Gas Turbine Demonstration Engine Program Review*, Metals and Ceramics Information Center, MCIC-78-36, March 1978, p. 517.
- <sup>4</sup>Hudson, D. A., "Problems and Promises in Gas Turbine Combustor Design Development," *Gas Turbine Combustor Design Problem*, edited by A. H. Lefebvre, 1980.
- <sup>5</sup>Mongia, H. C., Reynolds, R. S., Coleman, E., and Bruce, T. W., "Combustor Design Criteria Validation, Volume II—Development Testing of Two Full-Scale Annular Gas Turbine Combustors," USARTL-TR-78-55B, Feb. 1979.
- <sup>6</sup>Mongia, H. C. and Reynolds, R. S., "Combustor Design Criteria Validation, Volume III—User's Manual," USARTL-TR-78-55C, Feb. 1979.
- <sup>7</sup>Mongia, H. C. and Reider, S. B., "Allison Combustion Research and Development Activities," AIAA Paper 85-1402, 1985.
- <sup>8</sup>Fear, J. S., "The NASA Pollution-Reduction Technology Program for Small Aircraft Engines—A Status Report," AIAA Paper 76-616, 1976.
- <sup>9</sup>Mongia, H. C., Coleman, E. B., and Bruce, T. W., "Design and Testing of Two Variable-Geometry Combustors for High-Altitude Propulsion Engines," AIAA Paper 81-1389, 1981.
- <sup>10</sup>Dins, C. R., Evershed, R. J., Mongia, H. C., and Wimmer, J., "Advanced Material Segmented Combustor, Phase II, Interim Report," AFWAL-TR-80-2065, July 1980.
- <sup>11</sup>Johnson, K. P., Coleman, E. B., Smyth, J. R., and Lane, A. D., "Advanced Material Segmented Combustor Program," AFWAL-TR-83-2036, May 1983.
- <sup>12</sup>Sanborn, J. W., Mongia, H. C., and Kidwell, J. R., "Design of a Low-Emission Combustor for an Automotive Gas Turbine," AIAA Paper 83-338, 1983.
- <sup>13</sup>Bruce, T. W., Mongia, H. C., and Reynolds, R. S., "Combustor Design Criteria Validation, Volume 1—Element Tests and Model Validation," USARTL-TR-78-551, March 1979.
- <sup>14</sup>Srinivasan, R., et al., "Aerothermal Modeling Program, Phase I, Final Report, NASA CR-168243, Nov. 1983.
- <sup>15</sup>Srinivasan, R. and Mongia, H. C., "Numerical Computations of Swirling Recirculating Flow Final Report," NASA CR-165196, 1980.
- <sup>16</sup>Srivatsa, S. K., "Computations of Soot and  $\text{NO}_x$  Emissions from Gas Turbine Combustors," NASA CR-167930, 1982.
- <sup>17</sup>Patankar, S. V. and Spalding, D. B., *Heat and Mass Transfer in Boundary Layers*, Intertext Books, London, 1970.
- <sup>18</sup>Watts, K. C. and Brundrett, E., "Turbulence and Momentum Properties of Zero Pressure Gradient Boundary Layers with Suction on a Flat Plate," *Turbulent Boundary Layers*, edited by H. E. Weber, ASME, New York, 1979.
- <sup>19</sup>Emery, A. F. and Gessner, F. B., "The Numerical Prediction of the Turbulent Flow and Heat Transfer in the Entrance Region of a Parallel Plate Duct," ASME Paper 76-HT-39, Aug. 1976.
- <sup>20</sup>El Telbany, M. M. M. and Reynolds, A. J., "The Structure of Turbulent Plane Couette Flow," *Journal of Fluids Engineering, Transactions of ASME*, Vol. 104, Sept. 1982, p. 367.
- <sup>21</sup>Barbin, A. R. and Jones, J. B., "Turbulent Flow in the Inlet Region of a Smooth Pipe," *Journal of Basic Engineering, Transactions of ASME*, Vol. 85, March 1963, pp. 29-33.

- <sup>22</sup>Laufer, J., "The Structure of Turbulence in Fully Developed Pipe Flow," NACA Rept. 1174, 1954.
- <sup>23</sup>Saiy, M. and Peerless, S. J., "Measurement of Turbulence Quantities in a Two-Stream Mixing Layer," *Journal of Fluid Mechanics*, Vol. 89, 1978, pp. 709-722.
- <sup>24</sup>Champagne, F. H. and Wagnanski, I. J., "Coaxial Turbulent Jets," Boeing Scientific Research Laboratories, Rept. DI-82-0958, Feb. 1970.
- <sup>25</sup>Wagnanski, I. and Fiedler, M., "Some Measurements in a Self-Preserving Jet," *Journal of Fluid Mechanics*, Vol. 38, Pt. 3, 1969, pp. 577-612.
- <sup>26</sup>Charnay, G., Schon, J. P., Alcaraz, E., and Mathieu, J., "Thermal Characteristics of a Turbulent Boundary Layer with Inversions of Wall Heat Flux," *Proceedings of the 1st Symposium on Turbulent Shear Flows*, Vol. 1, 1977, pp. 15-47.
- <sup>27</sup>Hautman, D. J., Dryer, F. L., Schug, K. P., and Glassman, I., "A Multiple-Step Overall Kinetic Mechanism for the Oxidation of Hydrocarbons," *Combustion Science and Technology*, Vol. 25, 1981, pp. 219-235.
- <sup>28</sup>Cushing, B. S., Faucher, J. E., Gandbhir, S., and Shipman, C. W., "Turbulent Mass Transfer and Rates of Combustion in Confined, Turbulent Flames, II," *Eleventh Symposium (International) on Combustion*, The Combustion Institute, Pittsburgh, PA, 1967, pp. 817-824.
- <sup>29</sup>Mitchell, R. E., Sarofim, A. F., and Clomberg, L. A., "Experimental and Numerical Investigation of Confined Laminar Diffusion Flames," *Combustion and Flame*, Vol. 37, 1980, pp. 227-244.
- <sup>30</sup>Hassan, M.M.A., Lockwood, F. C., and Moneib, H. A., "Fluctuating Temperature and Mean Concentration Measurements in a Vertical Turbulent Free Jet Diffusion Flame," Imperial College, London, Rept. FS/80/21, 1980.
- <sup>31</sup>Shivaprasad, B. G. and Ramapriyan, B. R., "Turbulence Measurements in Boundary Layers Along Mildly Curved Surfaces," *Journal of Fluids Engineering, Transactions of ASME*, Vol. 100, 1978, pp. 37-46.
- <sup>32</sup>Kim, J., Kline, S. J., and Johnston, J. P., "Investigation of Separation and Reattachment of a Turbulent Shear Layer: Flow Over a Backward-Facing Step," ThermoSciences Div., Dept. of Mechanical Engineering, Stanford University, Stanford, CA, Rept. MD-37, 1978.
- <sup>33</sup>Eaton, J. K. and Johnston, J. P., "Turbulent Flow Reattachment: An Experimental Study of the Flow and Structure Behind a Backward-Facing Step," ThermoSciences Div., Dept. of Mechanical Engineering, Stanford University, Stanford, CA, Rept. MD-39, 1980.
- <sup>34</sup>Phataraphruk, P. and Logan, E., "Turbulent Pipe Flow Past a Rectangular Roughness Element," *Turbulent Boundary Layers, Forced, Incompressible, Nonreacting*, ASME, New York, June 1979, pp. 187-196.
- <sup>35</sup>Moon, L. F. and Rudinger, G., "Velocity Distribution in an Abruptly Expanding Circular Duct," *Journal of Fluids Engineering, Transactions of ASME*, 1977, pp. 226-230.
- <sup>36</sup>Fujii, S., Gomi, M., and Eguchi, K., "Cold Flow Tests of a Bluff-Body Flame Stabilizer," *Journal of Fluids Engineering, Transactions of ASME*, Vol. 100, 1978, pp. 323-332.
- <sup>37</sup>Lightman, A. J. et al., "Velocity Measurement in a Bluff-Body Diffusion Flame," AIAA Paper 80-1544, July 1980.
- <sup>38</sup>Johnson, B. V. and Bennett, J. C., "Mass and Momentum Turbulent Transport Experiments with Confined Coaxial Jets," NASA CR-165574, Nov. 1981.
- <sup>39</sup>Pitz, R. W. and Daily, J. W., "Experimental Study of Combustion in a Turbulent Free Shear Layer Formed at a Rearward Facing Step," AIAA Paper 81-0106, 1981.
- <sup>40</sup>Schefer, R. W. and Sawyer, R. F., "Pollutant Formation in Fuel Lean Recirculating Flows," NASA CR-2785, 1976.
- <sup>41</sup>Lewis, M. H. and Smoot, L. D., "Turbulent Gaseous Combustion, Part I: Local Species Concentration Measurements," *Combustion and Flame*, Vol. 42, 1973, pp. 277-285.
- <sup>42</sup>Morse, A. P., "Axisymmetric Free Shear Flows with and without Swirl," Ph.D. Thesis, University of London, England, 1980.
- <sup>43</sup>Unpublished work, Garrett Turbine Engine Co., Phoenix, AZ, 1973.
- <sup>44</sup>Unpublished work, Garrett Turbine Engine Co., Phoenix, AZ, 1981.
- <sup>45</sup>Brum, R. D. and Samuelsen, G. S., "Assessment of a Dilute Swirl Combustor as a Bench Scale, Complex Flow Test Bed for Modeling, Diagnostics, and Fuels Effects Studies," AIAA Paper 82-1263, 1982.
- <sup>46</sup>Janjua, S. I., McLaughlin, D. K., Jackson, T. W., and Lilley, D. G., "Turbulence Measurements in a Confined Jet Using a Six-Orientation Hot-Wire Probe Technique," AIAA Paper 82-1262, 1982.
- <sup>47</sup>Altgeld, H., Jones, W. P., and Whilhelmi, J., "Velocity Measurement in a Confined Swirl Driven Recirculating Flow," *Experiments in Fluids*, Vol. 1, 1983, pp. 73-78.
- <sup>48</sup>El-Banhawy, Y. and Whitelaw, J. H., "Experimental Study of the Interaction Between a Fuel Spray and Surrounding Combustion Air," *Combustion and Flame*, Vol. 42, 1981, pp. 253-275.
- <sup>49</sup>McGuirk, J. J., Taylor, A.K.M.P., and Whitelaw, J. H., "The Assessment of Numerical Diffusion in Upwind-Difference Calculations of Turbulent Recirculating Flows," Paper presented at Third Symposium on Turbulent Shear Flows, University of California, Davis, Sept. 1981.
- <sup>50</sup>Srinivasan, R., Berenfeld, A., and Mongia, H. C., "Dilution Jet Mixing Program, Phase I Report," NASA CR-168031, 1982.